DINAME 2023 - Proceedings of the XIX International Symposium on Dynamic Problems of Mechanics,
A.S. De Paula, A.T. Fabro and M.R. Machado (Editors), ABCM.
Pirenópolis, Go, Brazil, February 26th to March 3rd, 2023

Multi-element Polynomial Chaos in linear structures with nonlinear energy sink and uncertain parameters

Patricia Santana [1], Emmanuel Pagnacco [1], and Rubens Sampaio [2]

[1] Institut National des Sciences Appliquées de Rouen Normandie, Laboratoire de Mécanique de Normandie, BP 8, 76801 Saint Etienne du Rouvray Cedex, Rouen, France

[2] Pontifícia Universidade Católica do Rio de Janeiro, Mechanical Engineering Department, Avenida Marquês de São Vicente 255, Gávea, 22451-900, Rio de Janeiro, RJ, Brazil

Abstract: Coupling small nonlinear devices to principal mechanical system may allow to reduce vibrations of them by passive energy pumping phenomenon. The performance of the system is interesting considering the uncertainties, as a physical parameter of the system, in this case, the stiffness that makes the coupling between the systems. The objective of this paper is to give illustrative results and a discussion on the different numerical strategies when coupled non-linear dynamical systems with uncertain parameters are of interest, considering the Multi-element Polynomial Chaos Expansion strategy for their probabilistic model.

Keywords: Nonlinear Energy Sink, Polynomial Chaos, Uncertainty Quantification, Stochastic Process, Structural Dynamics

INTRODUCTION

Excessive vibrations in mechanical structures are one of the main reasons for their failure. The study of vibration reduction is thus of special interest to many engineering problems. Nonlinear energy sinks (NES) are passive nonlinear vibration dampers consisting of a spring mass damper with a strong nonlinear, usually cubic, stiffness. The NES can be adapted to the primary structure (PS) without the need to adjust to a specific frequency. Their operation is based on the concept of Targeted Energy Transfer (TET), which has become an important passive control technique to reduce or eliminate unwanted vibrations Snoun *et al*. (2022). Unlike linear dampers that have been widely studied over the years, the NES can act in a broadband fashion, producing a resonance capture cascade with a set of structural modes over a wide frequency range. According to Luz *et al.* (2015) the NES can be defined as a passive, adaptive, broadband boundary controller. However, the addition of the NES introduces degeneracies in the free and forced dynamics of the integrated system, opening the possibility of higher co-dimensional bifurcations and complex dynamic phenomena.

On the other hand, solving physical problems by converting them into a deterministic mathematical model can be considered a far-from-realistic approximation: considering the parameters as deterministic can lead to errors in the observed results. To overcome this problem, we introduce a possible randomness in parameters that can influence responses of the mechanical systems. One of the most famous and classical methods to solve this type of stochastic problem is the direct Monte-Carlo simulation (MCS), but it can require a lot of computational resources for problems of large sizes and several random variables. Another well-known method in the literature to solve this type of problem is the sensitivity-based analysis, such as the enhanced perturbation methods Dessombz (2000), but these methods have a limited radius of convergence and do not easily lead to statistical distributions of the results. Because of this, the study of spectral methods, such as the expansion in a polynomial basis of chaos (PC) Spanos *et al*. (1990), arises with the objective to obtain a representation model for the stochastic responses of a mechanical system.

In this paper, we focus on the stochastic processes of non-linear dynamics responses of mechanical systems equipped with NES, when random variables with known distributions are considered in their parameters. For dynamic systems, it appears that stochastic responses become highly nonlinear for a moderate to the high normalized coefficient of variation. Under these conditions, the representation of the output stochastic processes can be very difficult when using the chosen basis for the input variable, as is done in a basic implementation of the polynomial chaos method. Therefore, we investigate the multi-element polynomial chaos expansion (MPCE) Wan *et al*. (2005) to deal with this problem, as it appears as an attractive variant to represent the specific responses of these systems, in the sense that it is supposed to deal with these situations with less numerical difficulty thanks to an order of expansion kept low by adding more smaller elements Pagnacco *et al*. (2013).

In practice, two main strategies exist to determine the polynomial coefficients of the representation model: non-intrusive and intrusive. Considering first the non-intrusive strategy from a reference point of view, Snoun *et al*, (2022) uses the multi-element for a mechanical system that has a NES. It allows them to determine the propensity of the system to undergo

a Harmless Steady-State Regime. In Bonnaire *et al*. (2021) the Kármán vortex street problem is addressed and it is claimed that a few polynomial expansion terms are enough to obtain a good representation of the solution. Also, Wan *et al*. (2013) has reached the same conclusion for the Kraichnan-Orszag problem. But Chouvion *et al*. (2015) claims that it can be difficult to find a good quality of representation for a one-dimensional Duffing oscillator and the Kraichnan-Orszag three-mode problem with the multi-element strategy even for errors criteria basically based on the two first moments, mean and variance. Considering now the intrusive strategy in the literature, we can find reference Bonnaire *et al*. (2021) for unsteady Navier-Stokes problem with the asynchronous time integration (ATI-igPC), assuming that the frequency is a smooth function of the input variables. In this paper, only the mean and variance are considered to evaluate convergence. In Son *et al*. (2020), the non-intrusive and intrusive strategies are compared for different systems, among them nonlinear algebraic benchmark. In this case, the intrusive version is used in combination with a dimension reduction technique to obtain a computational efficiency over the non-intrusive version. In Ghorbaniasl *et al*. (2010), computational fluid dynamics applications are considered, comparing cumulative distribution function (CDF) of both strategies. In Pagnacco *et al*. (2013) difficulties in PC convergence for dynamical systems are shown. Both strategies are handled for the dynamic response of a linear mechanical system where it is proposed the use of two bases, one for the input parameters and another one for the output parameters to increase the robustness of the strategy. In this paper, Wasserstein's L_2 metric is used to evaluate the representation quality with a strong threshold error acceptance. This makes it possible to detect observable discrepancies in errors of the empirical probability density function (PDF) errors whereas no visible difference would be seen from the empirical CDF (due to the smoothing induced by the integration operation, thinking about its link with the PDF). This is definitely more stringent that observing the time evolution of the first two moments. In Jacquelin *et al*. (2015), complementary explanations are given for convergence difficulties that arise specifically for the intrusive approach when considering linear systems.

In this paper, the generalized and multi-element polynomial Chaos representation models are first recalled before presenting examples of numerical results. To deal with the proposed examples, reference result of the variability of the system responses is first estimated using the MCS associated with the sampling technique. Then, we consider a representation model obtained by a non-intrusive MPCE, before addressing it with an intrusive version to compare the results obtained by the two strategies with the help of an accurate distance measurement.

Generalized Polynomial Chaos Expansion

Polynomial expansions are generally used with the basic assumption that a finite sum of polynomials, often orthogonal polynomials, can accurately approximate a function of interest. In other words, it is a technique used to represent a random variable in terms of another variable with a known distribution. This strategy is widely used in modeling strategies or uncertainty propagation Xiu *et al*. (2003).

According to the Cameron-Martin theorem Xiu *et al*. (2002) the Wiener-Askey polynomial expansion of chaos can approximate and describe all stochastic processes with finite second-order momentum. This holds for most physical systems. Several classes of orthogonal polynomials are found in the Askey scheme, and their associated weighting functions are identical to the probability density function of associated distributions.

If we consider a generic model M with a single random variable ξ and a single output variable Z, the generalized polynomial chaos (gPC) expansion, is written:

$$Z = M(\xi) = \sum_{i=0}^{\infty} z_i \, \phi_i(\xi) \tag{1}$$

where $\phi_i(\xi)$ are the orthogonal polynomials which represent the stochastic part of the process, and z_i are the gPC coefficients that consider the deterministic part of the process. In this paper, uncertain parameters follow a uniform distribution and orthonormal Legendre polynomials are selected. The gPC theory states that for practical purposes the output variable of the system must be approximated by a truncated orthogonal polynomial, as follows:

$$Z \approx \sum_{i=0}^{n_z} z_i \, \phi_i(\xi) \tag{2}$$

where the number of terms $n_z + 1$ of the expansion is given by $n_z + 1 = \frac{(z+r)!}{z!r!}$ for r is the number of uncertain parameters and z the order of the gPC.

To determine the coefficients z_i we can find two main strategies in the literature: intrusive and non-intrusive. For the non-intrusive strategy, the coefficients are obtained by a dataset consisting of samples of the input random variable and the respective model evaluations. The main strategies to calculate these coefficients in a non-intrusive way are projection and regression.

Projection methods use the orthogonality of the basis functions to compute the coefficients by numerical integration, leading to:

$$z_i = \mathrm{E}[\phi_i(\xi)Z] \tag{3}$$

where E[ ] denotes the expectation operator. Regression methods formulate Eq. (1) as a system of linear equations and solve the system by standard linear regression approaches Wan *et al*. (2005). On the other hand, the intrusive strategy is closely related to the mechanical model of interest and follows a variational approach: Equation (1) is introduced into the mechanical model and the result is projected onto the chosen basis, supposed orthonormal, to determine the coefficients of the representation.

Multi-element Polynomial Chaos Expansion

When the system under consideration contains a nonlinear term, high polynomial orders for gPC may be necessary to reduce the approximation error. But another way is desirable as this leads to numerical difficulties. In the literature, the multi-element polynomial Chaos expansion (MPCE) was first introduced by Wan *et al*. (2005). It consists of defining a set of contiguous elements to describe the input variable and thus represent the response by a set of elements. This strategy consists of the decomposition of the random space and the construction of low-order orthogonal polynomials on each element that can be optimized by an adaptive procedure.

Let's start with partitioning the domain of definition $\mathcal{D}_\xi$ of the random variable ξ:

$$\mathcal{D}_\xi = \mathcal{D}_{\xi 1} \cup \mathcal{D}_{\xi 2} \cup \mathcal{D}_{\xi 3} \cup \ldots \cup \mathcal{D}_{\xi n} \tag{4}$$

where $\mathcal{D}_{\xi_j} = (d_{j-1},\, d_j)$ for all $j = \{1, 2, \ldots, n_c\}$. Consequently, a gPC expansion is developed in each element j as follows:

$$Z_j \approx \sum_{i=0}^{n_{z_j}-1} z_{i,j}\varphi_r(\xi_j) \tag{5}$$

where $Z_j(\xi_j)$ is the random process corresponding to the j-th element and an iso-probabilistic transformation is used

$$\mathcal{T}_{\xi j}(x) = P_{\xi j}^{-1}(P_\xi(x)) \text{ for } \xi_j(x) = \mathcal{T}_{\xi j}(x) \tag{6}$$

MPCE model for dynamic responses of mechanical systems and numerical implementation

Here, the generic mechanical model of interest $M(t)$ is time dependent. In this paper, it is expanded with the MPCE as follows:

$$Z_j(t) \approx \sum_{i=0}^{n_{z_j}-1} z_{i,j}(t)\varphi_r(\xi_j) \tag{7}$$

where the polynomial coefficients are obtained from a projection approach for the non-intrusive strategy or a variational approach for the intrusive strategy.

Example of numerical results

Simple single degree-of-freedom linear dynamical system

Let us first consider the stochastic initial value ordinary differential equation model problem:

$$\ddot{Z} + \xi^2 Z = 0 \;\text{ for } t \geq 0 \tag{8}$$

where $\ddot{Z} = \frac{\partial^2 Z}{\partial t^2}$, t denotes the time and $Z(t=0,\xi) = 1,\; Z'(t=0,\xi\,) = 0$. The solution of the equation is the stochastic process $Z(t,\xi) = \cos(\xi t)$ and we consider a uniform random variable $\xi \sim \mathcal{U}(0,1)$. For this problem, as it is generally known for stochastic dynamical systems, it is difficult to find a good statistical representation of the solution for long time. However, using the multi-element strategy, we can obtain a very good representation of the system solution.

First, we estimated the variability of the system responses by Monte-Carlo simulation (MCS) associated to the sampling technique. Calculating the response of the system with the sampling technique, the convergence of the response is found with 10^5 sample. Next, the uncertainty representation model is evaluated by the non-intrusive and the intrusive strategies using polynomial order 4 for each segment of 19 elements that have the same size. For both of them, we use the ordinary differential equation solver *ode113* of MATLAB.

As can be seen in Fig. 1, we are able to obtain a very good statistical representation of the displacement responses for a relatively high time of 30 seconds because no discrepancies are observable between MCS and MPCE results: In Fig. 1, the histogram of the random variable found from MCS is overlaid on the histograms of the variables found by MPCE. However, to quantitatively ensure the quality of the chaos representation and to be able to compare different results, we define an error indicator ϵ.

For this purpose, we use the Wasserstein's L_2 metric (Gelbrich 1990) which is a distance function between two probability measures P_1 and P_2. In our implementation, this metric is normalized by the variance of one variable, as follows:

$$\epsilon = \frac{\inf\{[\sqrt{\mathrm{E}(X_1 - X_2)^2}}{\mathrm{E}(X_1 - \mathrm{E}(X_1))^2} : \{\mathcal{L}(X_1) = P_1, \mathcal{L}(X_2) = P_2\} \tag{9}$$

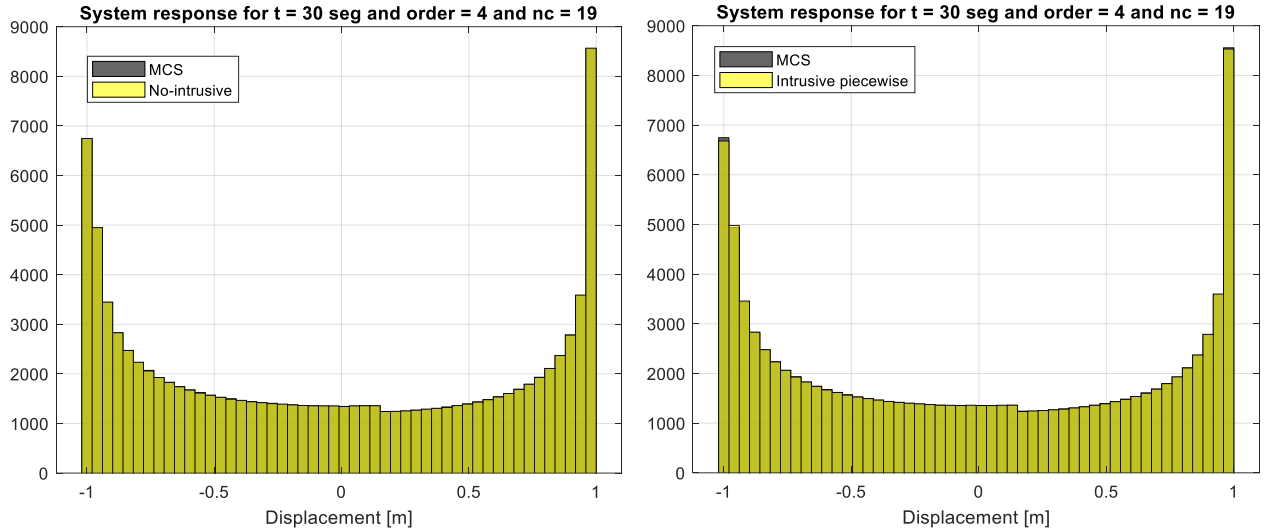

Figure 1. Comparison of the system's displacement statistics

where $\mathcal{L}(X)$ is the statistical law associated with the variable X. Since the Wasserstein metric is used to compare the probability distributions of two real variables X_1 and X_2, it can be used as an error indicator when one of the two random variables are considered as a reference. In the cases studied here, the distribution obtained by MCS will be the one considered for the random variable X_1 as the reference, to compare it with the result of X_2 obtained by multi-PCE. From the qualitative observations, we found that the numerical value of this indicator must be less than or equal to 1×10^{-3} to ensure a very good representation.

Applied to this example at the time $t = 30$ seconds, we get an error of 4.95×10^{-4} for the non-intrusive approach while it is 7.63×10^{-4} for the intrusive approach.

Two degree-of-freedom nonlinear dynamical system

We consider now the mass-spring-damper system of Gourdon *et al*. (2005). It is a two-degree-of-freedom (DOF) system composed of two weakly coupled and damped oscillators: a principal system (PS) and a nonlinear energy sink (NES), see Fig. 2.

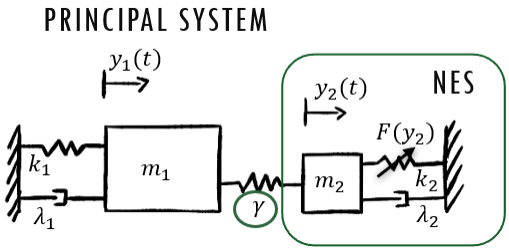

Figure 2. Design of a Mass-Spring-damper system with NES

Solutions of the problem are the displacements y_1 and y_2, and the equations of the complete system are as follows:

$$\begin{aligned} m_1\ddot{y}_1 + \lambda_1\dot{y}_1 + k_1 y_1 + \gamma(y_2 - y_1) &= 0 \\ m_2\ddot{y}_2 + \lambda_2\dot{y}_2 + k_2 y_2 + C y_2^{2n+1} + \gamma(y_1 - y_2) &= 0 \end{aligned} \tag{10}$$

with the initial conditions $y_1(0) = y_2(0) = \dot{y}_2(0) = 0$ and $\dot{y}_1(0) = \sqrt{2h}$. The fixed parameters of the system are:

$n = 2, m_1 = 1, m_2 = 0.1, k_1 = 0.9, k_2 = 0, C = 0.1, \lambda_1 = 0.05, \lambda_2 = 0.01$ and $h = 0.25$, while the coupling term γ is of special interest in this application.

Let us first get some insight into the mechanical behavior of the nominal system when $\gamma = 0.05$, in the context of the principal system vibration reduction. Fig. 3 reveals the energy transfer from the directly excited principal oscillator to the NES, after an initial transient state. Most of the vibrational energy is irreversibly transferred or "pumped" to the NES.

To determine the efficiency of this pumping, we set a very short t of 30 secondes to calculate the energy ratio between the linear and the nonlinear oscillator in this time. It is widely used in the literature that an "optimal" pumping will be determined when this energy ratio exceeds a level above 70%, which helps us to define a set of parameters at which we can consider this energy pumping optimal. Thus, the energy ratio is calculated as follows:

$$Ratio = \frac{E_{nes}(t = 30\ seg)}{E_{PS}(t = 30\ seg) + E_{nes}(t = 30\ seg)} \tag{11}$$

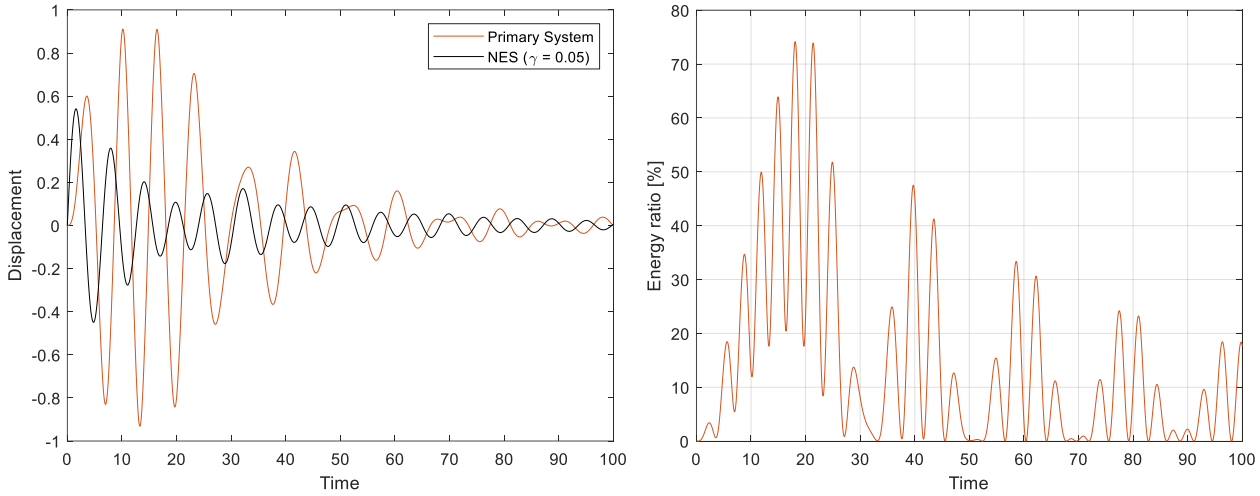

Figure 3. (a) Displacement of PS and PS-NES for $\gamma = 0.05$ and $h = 0.15$. (b) Energy ratio for $\gamma = 0.05$ and $h = 0.15$

Another way to analyze this energy pumping is through numerical wavelet transforms (WT), which can provide details of the frequency components of a signal during an analyzed time interval from the WT spectra. Fig. 4a reveals some interesting features of the system dynamics, knowing that the heavily shaded regions correspond to regions where the WT amplitude is high, while the lightly shaded regions correspond to low amplitudes. Indeed, we observe that a transient resonance capture (TRC) of the response dynamics is produced by a strongly nonlinear mode whose frequency varies in time and does not lie between the two natural frequencies of the uncoupled and undamped system, which are 0.107 and 0.159, which means that this mode is predominantly located in the nonlinear accessory.

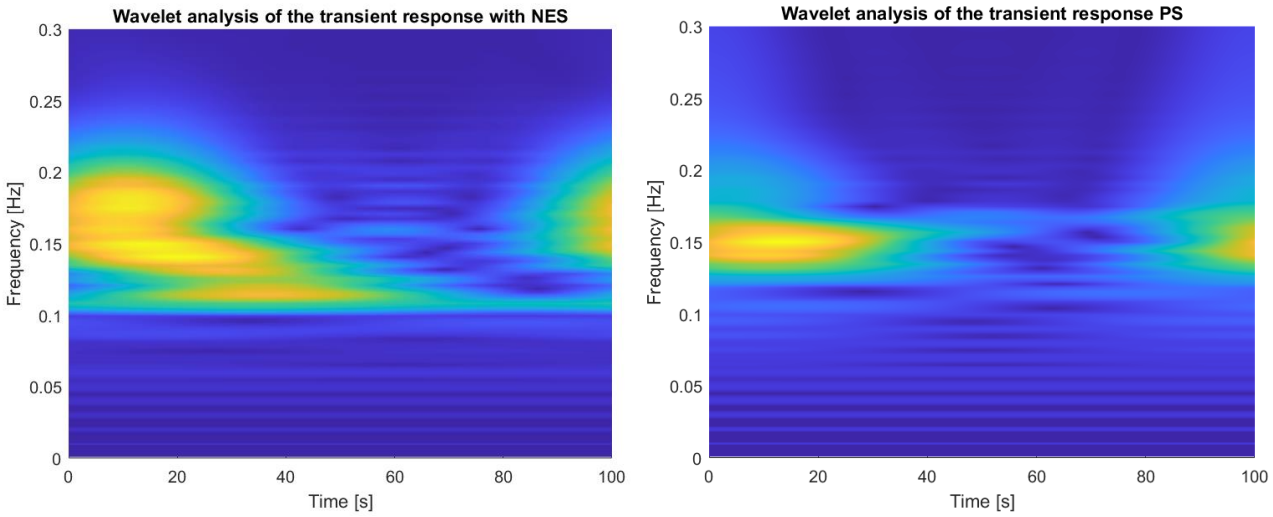

Figure 4. Wavelet analysis for the transient response

The strong nonlinearity of the response is also manifested by the appearance of an initial oscillation of multiple frequencies, and this can be seen by the existence of an initial high frequency component in the spectrum, Fig. 4a, while in Fig. 4b, it can be seen as there is no energy transfer. To summarize, these results indicate that in this case, with proper excitation, the strong energy transfer associated with the TRCs of the nonlinear attachment dynamics by strongly nonlinear modes that are predominantly located in the NES, moreover these TRCs take place over a wide frequency range, resulting in a broadband targeted energy transfer (TET).

For the stochastic problem, we consider the coupling term as the uncertain parameter $\gamma \sim \mathcal{U}(0.02\ ,0.2)$ in this system. As a consequence, the outputs (solutions) are stochastic processes. However, before addressing this stochastic problem, it is interesting to see the responses solutions for several deterministic values of γ, as seen in Fig. 5. Next, we numerically constructed a reference solution for this stochastic problem with the MCS approach. Unlike the previous example, 10000 samples were needed to find the convergence of the displacement distributions. Moreover, for this nonlinear system, we found it necessary to choose a high accuracy solver and we choose the *Implicit Runge-Kutta Radau* of 7th order. Fig. 6 shows the first and second statistical moments of the stochastic process $y_2(t)$.

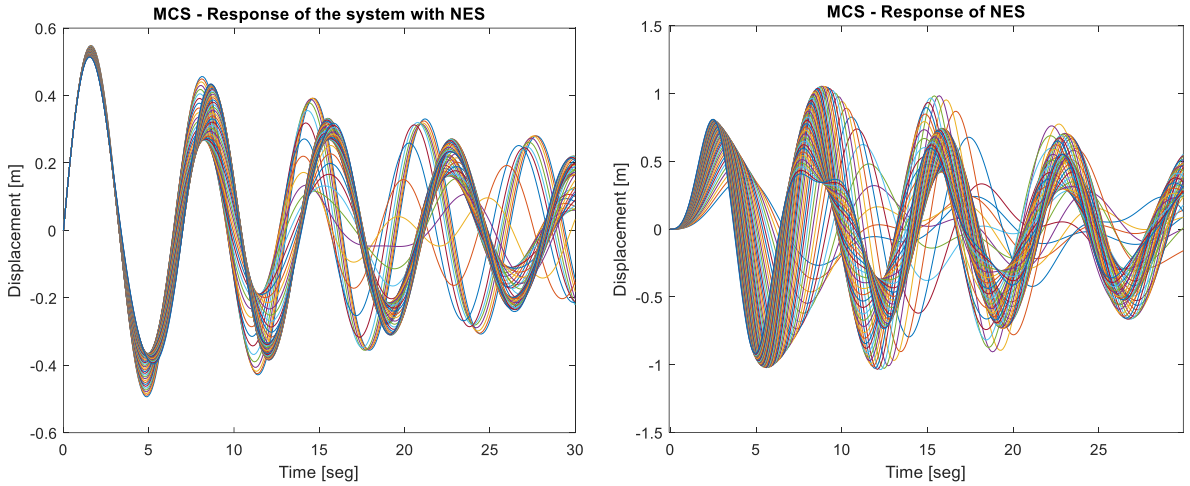

Figure 5. Variability of 50 responses produced by a linear sampled of deterministic values of γ: $y_1(t)$ (right), $y_2(t)$ (left)

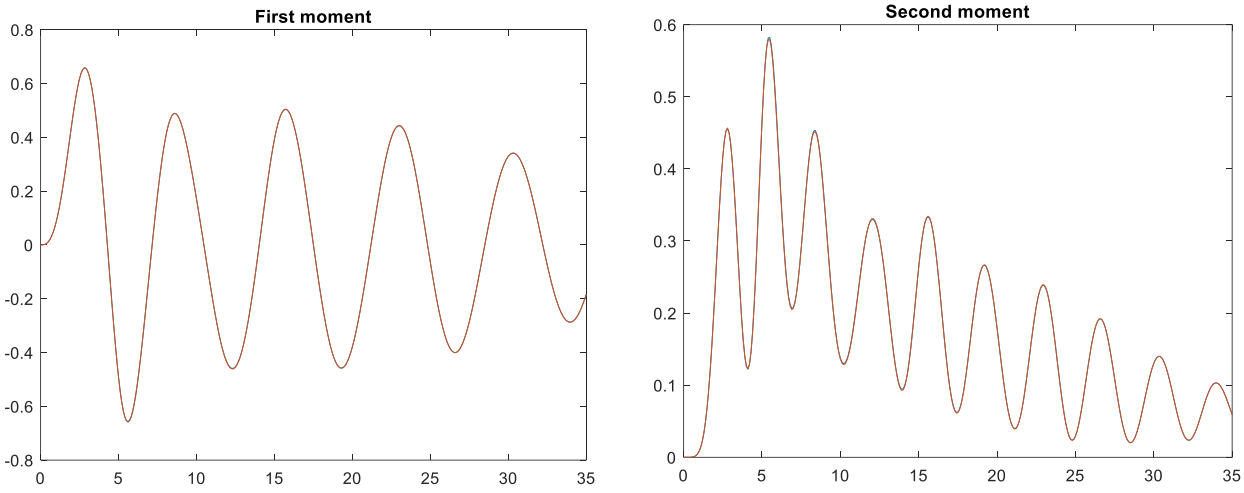

Figure 6. First statistical moments and second statistical moments of $y_2(t)$ for the 2 DOF nonlinear system

Fig. 7, the instantaneous time-varying histogram of this system is displayed for a time of 25 to 35 seconds, showing how variable the response of the system can be over time.

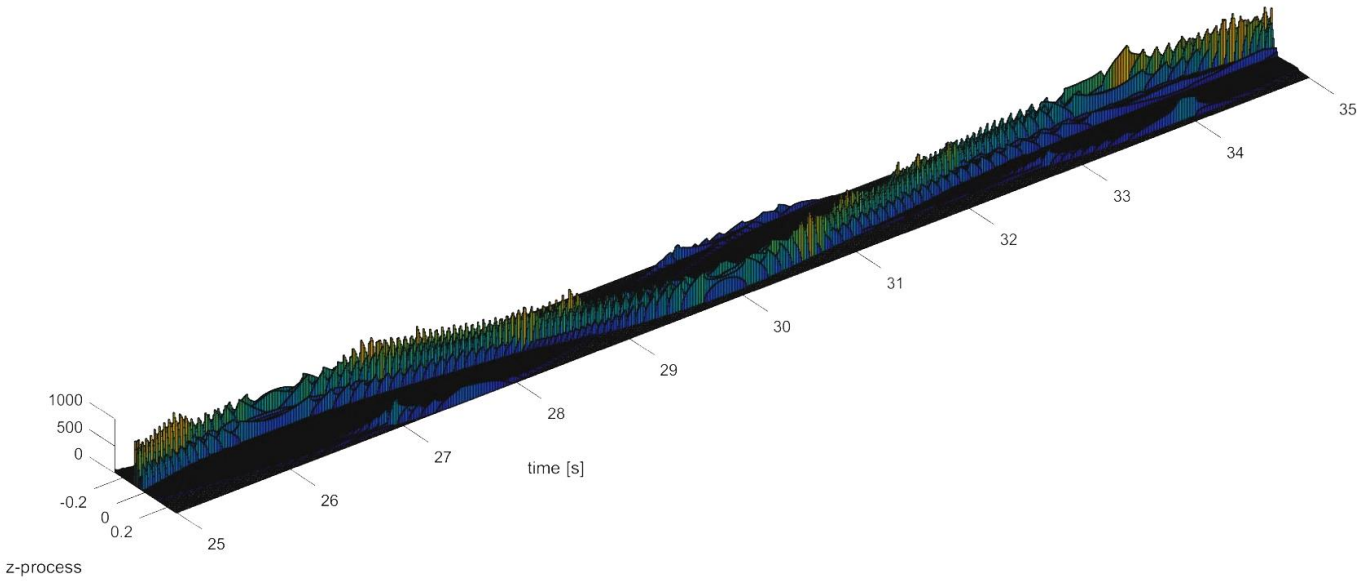

Figure 7. Instantaneous time-varying histogram of the system from MCS of the $y_1(t)$ stochastic process

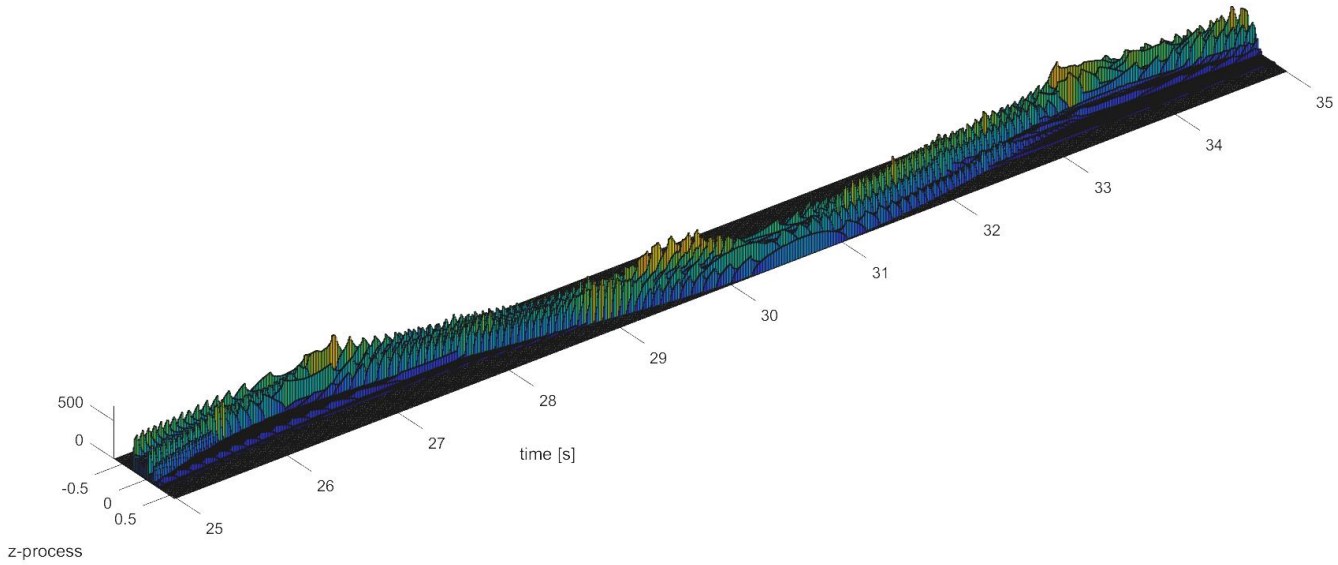

Figure 8. Instantaneous time-varying histogram of the system from MCS of the $y_2(t)$ stochastic process

Non-intrusive approach

In the first approach, we used the non-intrusive version of MPCE. As we have estimated the variability of the system response by MCS associated to the sampling technique, it becomes possible to use it as a data base for the evaluation of the coefficients. Fig. 9 show the results obtained at the arbitrary time $t = 30$ seconds. Although arbitrary, this time is chosen sufficiently long to assess the quality of the representation model while it corresponds to a high level of energy pumping and also to a high level of the second statistical moment. As can be seen in Fig. 9, despite the nonlinearity that the NES brings to the system, and the intrinsic nonlinearity of the NES, it is possible to reproduce the displacement distribution numerically constructed with the MCS using the MPCE in the non-intrusive version, although none of the distributions obtained resembles any known distribution. When applying the MPCE, in the first instance 350 elements of order 1 are considered for the model representation of $y_1(t)$, while for $y_2(t)$ 412 elements of order 1 were necessary to obtain this good approximation with 10000 samples.

Similar to the previous linear system, to quantify the quality of the representation, we calculate the Wasserstein's metric for a time of 30 seconds, since it allows us to verify that we do not have problems with the long time and the energy transfer in the system up to this time is the highest. For this strategy, this time complies with the numerical value of the error indicator of 4.98×10^{-4} for $y_1(t = 30)$ and 1.38×10^{-3} for $y_2(t = 30)$, ensuring a satisfactory representation.

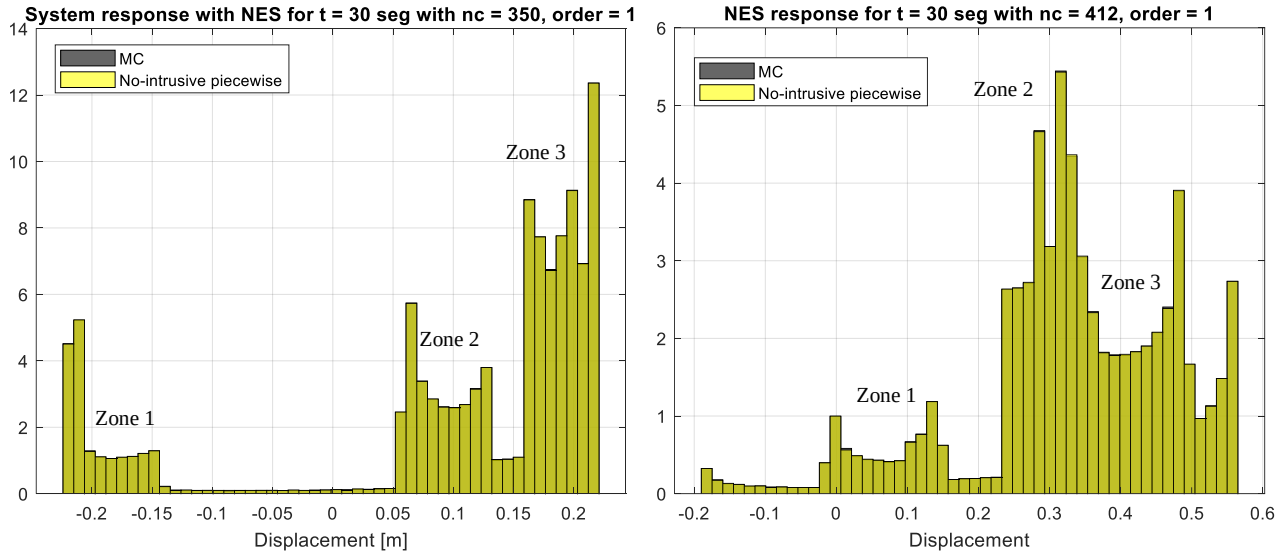

Figure 9. Normalized histogram response of the displacements for the MCS and MPCE using a non-intrusive strategy. (a) Primary system response with NES; (b) NES response

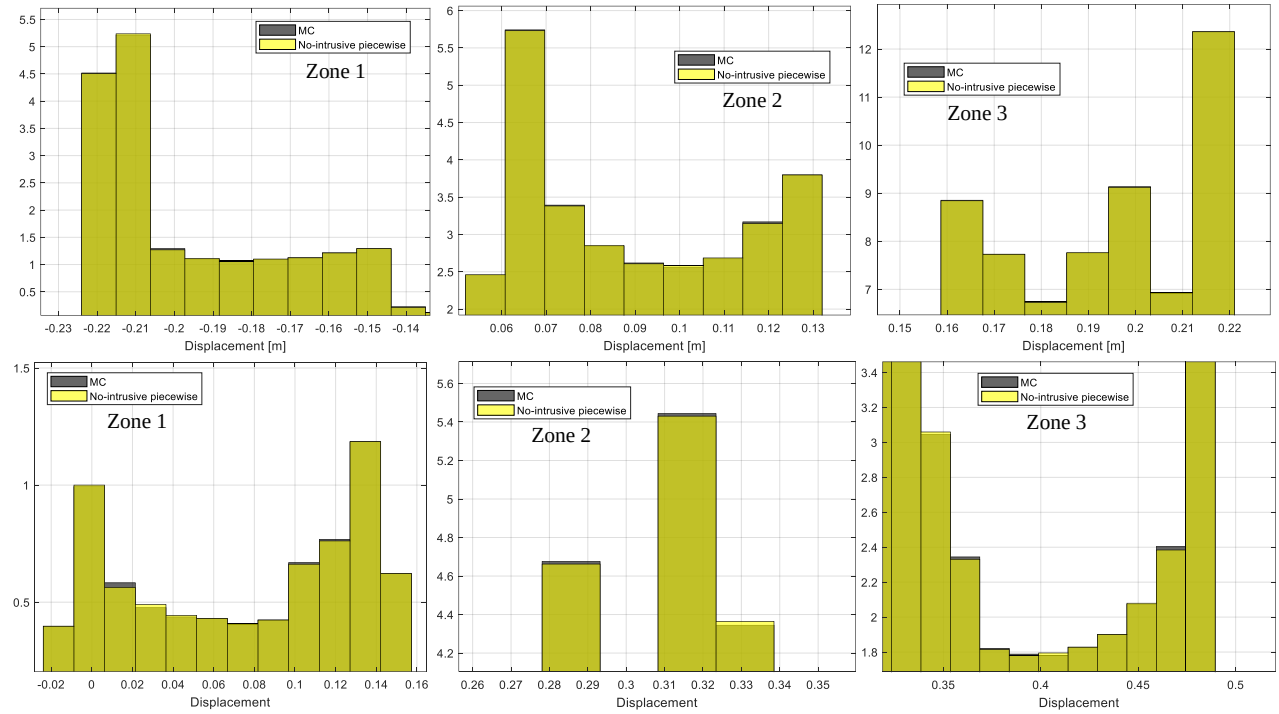

Figure 10. Zoom of normalized histogram response of the displacements for the MCS and MPCE using a non-intrusive strategy. (a) Primary system response with NES (the top three); (b) NES response (the three below).

Intrusive approach

A second approach is to analyze the representation found with the intrusive strategy, a strategy that is not as widely used as the non-intrusive strategy because it requires specific developments for each specific formulation of the problem.

Similar to the non-intrusive approach, a polynomial order of 1 and 350 elements is selected for y_1 an order 1 and 450 pieces for y_2 and 10000 samples. Fig. 11 shows the results obtained, as well as a comparison with the normalized MCS histogram for a time of 30 seconds. To quantify the quality of the response, the Wasserstein metric was also used, which gives 1.23×10^{-3} for $y_1(t = 30)$, and 6.90×10^{-3} for $y_2(t = 30)$. These results are almost as good as the one of the non-intrusive approach, while slightly more elements appear to be needed.

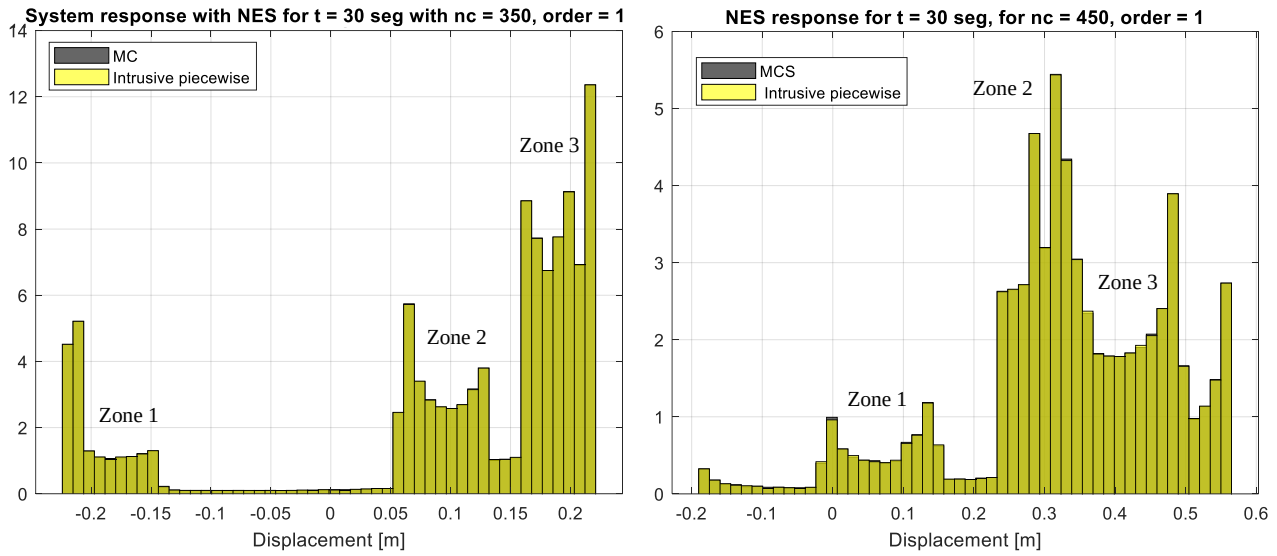

Figure 11. Normalized histogram responses of the displacements for the MCS and MPCE using an intrusive strategy. (a) Primary system response with NES; (b) NES response

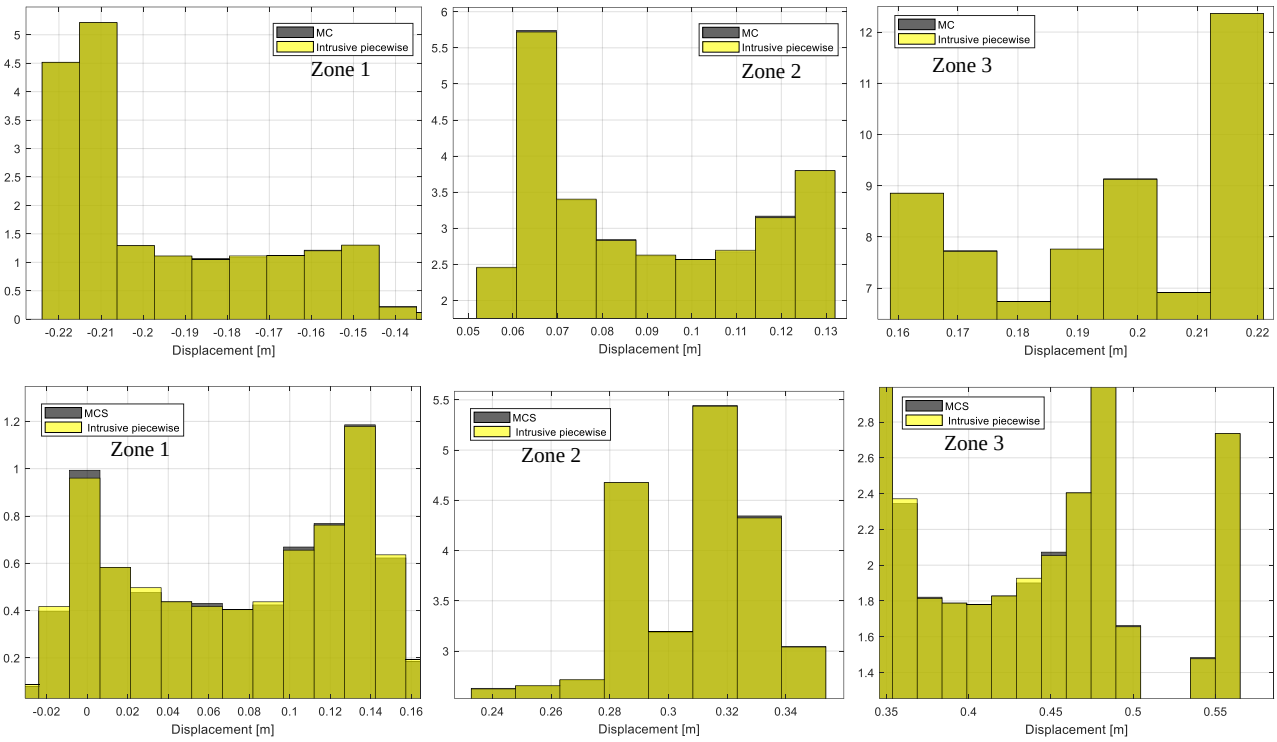

Figure 12. Zoom of normalized histogram response of the displacements for the MCS and MPCE using an intrusive strategy. (a) Primary system response with NES (the top three); (b) NES response (the three below).

CONCLUSIONS

In this paper, we have investigated the performance of the MPCE representation model for stochastic processes that arise with examples of linear and non-linear systems in structural dynamics. The first example is a linear SDOF system, where no major difficulties were obtained. As expected, the results are excellent, whether one considers the non-intrusive or intrusive strategy for finding the model coefficients. On the one hand, this observation is very logical because the representation model is uniquely fixed for this example, so when convergence of its parameters is obtained, the same results should be obtained regardless of the strategy chosen to evaluate them. This also highlight the fact that the representation model is good since it perfectly reproduces the reference data. On the other hand, it is worth mentioning that these good results are obtained under the simplest conditions with few strategic efforts because the basis selected is the one that best fits the input random variable, while a relatively low polynomial order is chosen on the elements and while a not-adapted but uniform element size is chosen.

Next, we proposed to investigate a more complex system having 2-DOF and a NES. To better understand its behavior, we first studied the reduction of the vibration quantified by the energy ratio and present its wavelet spectra. In this first result we observe that the energy transfer from a linear system to a nonlinear system can be optimal for certain parameters. In this system, the parameters are selected to achieve a strong energy transfer from linear to nonlinear system thanks to the fact that the predominant nonlinear modes are those found in the NES, so that the TRC occurs over a wide frequency range, which means that the energy transfer occurs at various frequencies.

Then, the representation model of the stochastic displacements of the non-linear dynamical system composed of the PS and the NES is investigated, both with the non-intrusive and intrusive strategies. The non-intrusive strategy yields coefficients that give good results by the model. Not surprisingly, this nonlinear example suffers from a slower convergence of the MPCE compared to the linear example, since more elements are needed, but, in spite of this, good results are obtained with a representation model formed by basic polynomials of low order and despite the fact that the size of the elements remains uniform and does not adapt. To reach these results, it was necessary to change the solver from ode113 to Radau. Moreover, a few more elements are needed with the intrusive strategy.

Finally, it is worth noting the error indicator that we use here to evaluate the quality of the representation. Indeed, it allows a relevant numerical quantification of what may be only slightly visible from the histograms, whereas no error would be visible by plotting only the first statistical moments or even the empirical CDFs of MPCE superimposed on those of MCS.

REFERENCES

Bell, J. (2015). The Cameron-Martin theorem. *Department of Mathematics, University of Toronto*, pp. 1-9.

Bonnaire, P., Pettersson, P., & Silva, C. F. (2021). Intrusive generalized polynomial chaos with asynchronous time integration for the solution of the unsteady Navier–Stokes equations. *Computers and Fluids, 223*, pp. 1-15.

Chouvion, B., & Sarrouy, E. (2015). Development of error criteria for adaptive multi-element polynomial. *Mech. Syst. Signal Process.*, pp. 1-37. doi:, http://dx.doi.org/10.1016/j.ymssp.2015.05.007i

Dessombz, O. (2000). Analyse dynamique de structures comportant des paramètres incertains. *PhD thesis, Ecole Centrale de Lyon*, pp. 1-161.

Gelbrich, M. (1990). On a Formula for the L2 Wasserstein Metric between Measures on Euclidean and Hilbert Spaces. *Mathematische Nachrichten*, pp. 185-203. doi:10.1002/mana.19901470121

Ghorbaniasl, G., Bijl, H., Lacor, C., Pereira, J. C., Sequeira, A., Onorato, G., . . . Bijl, H. (2010). Comparison of intrusive and non-intrusive polynomial chaos methods for CFD applications in aeronautics. pp. 1-16.

Gourdon, E., & Lamarque, C. H. (2005). Energy Pumping with Various Nonlinear Structures: Numerical Evidences. *Nonlinear Dynamics*, pp. 281-307.

Jacquelin, E., Adhikari, S., Sinou, J.-J., & Friswell, M. (2015). Polynomial Chaos Expansion and Steady-State Response of a Class of Random Dynamical Systems. *Journal of Engineering Mechanics - ASCE, American Society of Civil Engineers*, pp. 4-16.

Luz, S., & Toro, Y. (2015). *Nonlinear Targeted Energy Transfer in Mechanical and Structural Systems.* Springer.

Pagnacco, E., Sarrouy, E., Sampaio, R., & Souza de Cursi, E. (2013). Polynomial chaos for modeling multimodal dynamical systems-Investigations on a single degree of freedom system. *Mecánica Computacional*, pp. 705-727.

Snoun, C., Bergeot, B., & Berger, S. (2022). Robust optimization of nonlinear energy sinks used for mitigation of friction-induced limit cycle oscillations. *European Journal of Mechanics, A/Solids, 93*, pp. 1-13.

Son, J., & Du, Y. (2020). Comparison of intrusive and nonintrusive polynomial chaos expansion-based approaches for high dimensional parametric uncertainty quantification. *Computers and Chemical Engineering, 134*, pp. 1-12.

Spanos, P., & Ghanem, R. (1990). Polynomial Chaos in Stochastic Finite Elements. *Journal of Applied Mechanics*, pp. 197-202.

Wan, X., & Karniadakis, G. (2005). An adaptive multielement generalized polynomial chaos method. *Journal of Computational Physics*, pp. 617-642.

Wan, X., & Karniadakis, G. (2013). Multi-element generalized polynomial chaos for arbitray probability measures. *2006 Society for Industrial and Applied Mathematics*, pp. 901-928.

Xiu, D., & Karniadakis, G. E. (2002). The Wiener–Askey polynomial chaos for stochastic differential equations. *Society for Industrial and Applied Mathematics*, pp. 619-644.

Xiu, D., Lucor, D., Su, C., & Karniadakis, G. (2003). Performance evaluation of generalized polynomial chaos. *Computational Science ICCS 2003*, pp. 346-354.